

Detection of SO towards the transitional disk AB Auriga: the sulfur chemistry in a proto-solar nebula¹

Asunción Fuente¹, Marcelino Agúndez², José Cernicharo², Javier R. Goicoechea² and Rafael Bachiller¹

¹ Observatorio Astronómico Nacional (OAN), Apdo 112, E-28803 Alcalá de Henares, Madrid, Spain

² Instituto de Ciencia de Materiales de Madrid, ICMM-CSIC, C/ Sor Juana Inés de la Cruz 3, E-28049 Cantoblanco, Spain

Abstract

The transitional disk around the Herbig Ae star, AB Auriga, has been imaged in the dust continuum emission at 1mm and in the line using the NOEMA interferometer (IRAM) (beam $\sim 1.5''$). This is the first image of SO ever in a protoplanetary disk (PPD). Simultaneously, we obtained images of the ^{13}CO 2 \rightarrow 1, C^{18}O 2 \rightarrow 1 and H_2CO 3 $_{0,3}$ \rightarrow 2 $_{0,2}$ lines. The dust continuum and C^{18}O emissions present the horseshoe morphology that is characteristic of the existence of a dust trap, proving that this disk is at the stage of forming planets. In contrast, SO presents uniform emission all over the disk. We interpret that the uniform SO emission is the consequence of the SO molecules being rapidly converted to SO_2 and frozen onto the grain mantles at the high densities close to the disk midplane ($> 10^7 \text{ cm}^{-3}$). SO is the second S-bearing molecule detected in a PPD (the first was CS) and opens the possibility to study the sulphur chemistry in a proto-solar nebula analog. Sulfur is widespread in the Solar System and the comprehension of the sulfur chemistry is of paramount importance to understand the formation of our planetary system.

1 Introduction

The comprehension of chemistry in disks is an important step to understand the formation of complex organic, even prebiotic molecules, on planets. However, the disk chemistry is a very

¹Based on observations carried out under project number S14AO with the IRAM NOEMA Interferometer. IRAM is supported by INSU/CNRS (France), MPG (Germany) and IGN (Spain)

unexplored field from the observational point of view with very few molecular detections. This is mainly due to the low molecular abundances in the gas disk, because of the intense UV radiation from the central star and the freeze out of the molecules onto dust grains. This scarcity of molecules seems more accentuated in disks around Herbig Ae stars [8]. Recently, [9] carried out a molecular search towards the transitional disk AB Auriga (hereafter, AB Aur) using the IRAM 30-m telescope. As a result, they detected the several lines of CO and its isotopologues, HCO^+ , H_2CO , HCN, CN, and CS lines. In addition, they detected two 1mm SO lines which confirmed previous tentative detection of this species by [6]. AB Aur is the only protoplanetary disk (PPD) detected in SO thus far, and its detection is consistent with the interpretation of this disk being warmer and younger than those associated with T Tauri stars.

Transitional disks are objects around young stars with large cleared cavities in the inner disk regions. The formation of planetesimals requires that primordial dust grains grow from micron- to km-sized bodies. Lopsided dust distributions have been commonly identified in transitional disks using the dust continuum emission at millimeter wavelengths [5]. Asymmetrical structures tend to be formed when dust grains become trapped in a high gas density vortex potentially promoting rapid growth to the planetesimal scale. As the consequence, a lower gas-to-dust mass ratio and larger grains are expected within the dust trap. Dust traps are exciting features that could be related to protoplanets buried in the disk. The study of the gas chemical evolution in the dust trap is of paramount importance for planet formation studies.

2 AB Auriga

Our target, AB Aur, is one of the best-studied Herbig Ae stars and hosts a prototypical Herbig Ae disk. It has a spectral type A0-A1 [7], a stellar mass of $M_\star \sim 2.4 M_\odot$, $T_{\text{eff}} \sim 9500$ K, and is located at a distance of 145 pc [3]. The disk around AB Aur shows a complex structure, quite different from those observed in disks around T Tauri stars. It is larger ($R_{\text{out}} \sim 1100$ AU, $\approx 7''$) and shows spiral-arm features clearly traced by the molecular emission [14].

On the basis of interferometric observations of ^{12}CO and its isotopologues using the Plateau de Bure Interferometer (PdBI), [11] found that, contrary to typical disks associated with TTs, the AB Aur disk is warm (>25 K all across the disk) and shows no evidence of CO depletion. More recently, [6] and [9] carried out a molecular search using the IRAM 30-m telescope. As a result, they detected a few molecules common in PPDs and three millimeter lines of sulfur monoxide (SO). SO had never been detected before in a T Tauri or Herbig Ae disk and its detection provided further support to the interpretation of a warmer chemistry in this kind of Herbig Ae disk. However, there are some observations that suggest the possibility that the SO emission could be coming from an outflow or from an envelope rather than from the circumstellar disk and this detection required of interferometric confirmation.

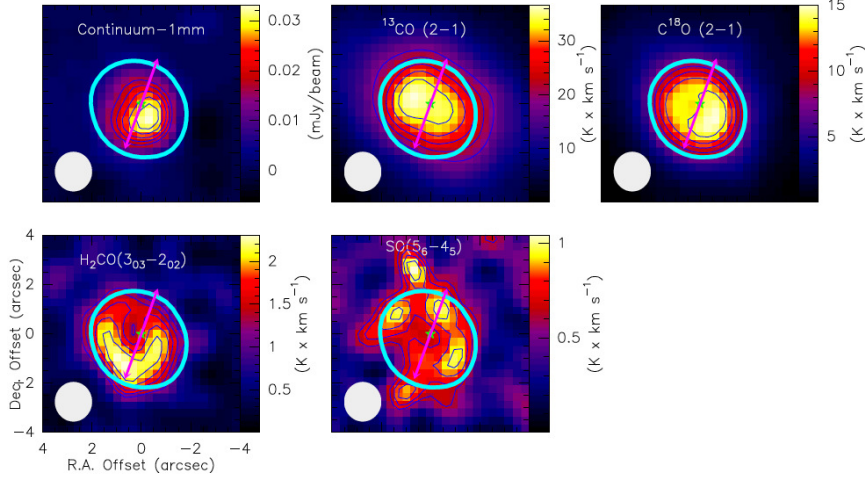


Figure 1: NOEMA images of the circumstellar disk around AB Aur [10]. White ellipses at the bottom-left corner of each panel represents the beam size ($\sim 1''.6 \times 1''.5$). The thick blue contour indicates the 50% level of the $C^{18}O$ emission. The arrow marks the direction of the ionized jet [12].

3 Observations and results

The interferometric observations were carried out with the NOEMA interferometer in CD configuration on March 2015 with 6 antennas providing the angular resolution of $1''.6 \times 1''.5$. We targeted AB Aur ($\alpha_{J2000}=04h\ 55m\ 45.8s$, $\delta_{J2000}=30^\circ\ 33'\ 04''.2$) to observe simultaneously the H_2CO $J=3_{0,3} \rightarrow 2_{0,2}$ line at 218.222 GHz, the SO $J=5_6 \rightarrow 4_5$ line at 219.949 GHz, the $C^{18}O$ $J=2 \rightarrow 1$ line at 219.560 GHz, and the ^{13}CO $J=2 \rightarrow 1$ line at 220.398 GHz. The channels free of line emission were used to estimate the continuum flux that was subtracted from the spectral maps. To improve the S/N, all maps were created with a velocity resolution of $0.25\ km\ s^{-1}$. We used 3C84, 3C454.3, MWC349, J0433, and J0418 as phase and flux calibrators. Data reduction and image synthesis were carried out using the GILDAS software.

Fig.1 shows the NOEMA images of the dust continuum emission and the ^{13}CO $J=2 \rightarrow 1$, $C^{18}O$ $J=2 \rightarrow 1$, H_2CO $J=3_{0,3} \rightarrow 2_{0,2}$ and SO $5_6 \rightarrow 4_5$ lines. The dust continuum emission reveals the horseshoe morphology characteristic of the existence of a dust trap. The emission of the molecular lines coincides with the ring detected in the dust continuum emission, but significant differences exist among their azimuthal spatial distributions. The asymmetry observed in the continuum emission seems smeared in the map of the ^{13}CO $J=2 \rightarrow 1$ line. This is not surprising since this line is optically thick and it is mainly tracing the gas temperature at an intermediate gas layer between the disk surface and the equatorial plane. The spatial distribution of the $C^{18}O$ $J=2 \rightarrow 1$ line is very similar to that of the dust continuum emission. In fact, the ratio between 1mm continuum and $C^{18}O$ $J=2 \rightarrow 1$ emission ($1mm\ continuum / (C^{18}O\ 2 \rightarrow 1)$) is uniform in the disk within a factor of ~ 1.3 . Taking into account the uncertainties in the dust temperature and dust opacities, we consider that there is no evidence that the gas-to-dust mass ratio varies inside the dust trap. We cannot discard possible variations of the

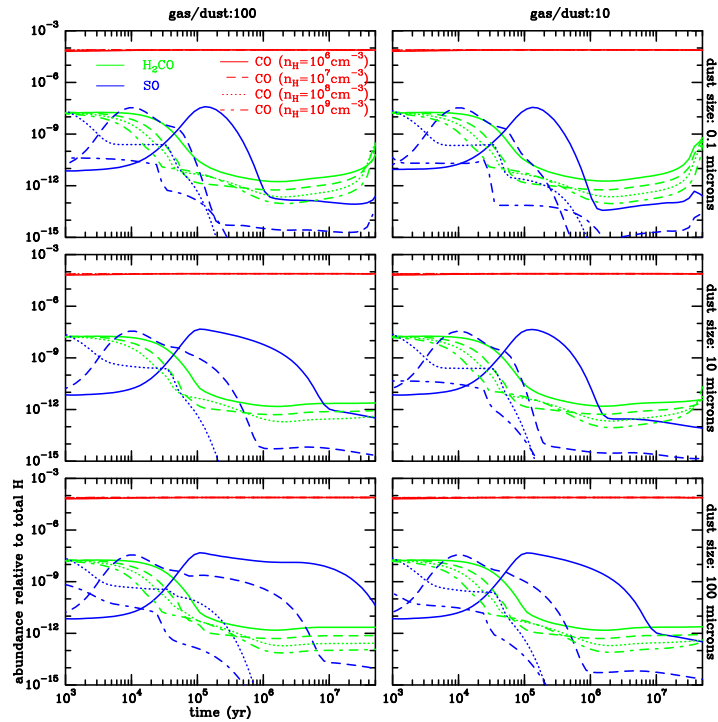


Figure 2: Chemical model abundance results. Predicted CO, H₂CO, and SO fractional abundances as a function of time for different molecular hydrogen densities, gas-to dust mass ratios, and grain sizes [10].

gas-to-dust mass ratio at smaller scales ($\ll 230$ AU) that are not detected with the angular resolution of our observations. The H₂CO J=3_{0,3} \rightarrow 2_{0,2} emission peak is coincident with the dust trap defined by the 1mm continuum and the C¹⁸O J=2 \rightarrow 1 emissions, but extends further away toward the south. The SO J=5₆ \rightarrow 4₅ line presents an almost uniform emission along the ring, with an enhancement toward the northeast.

Remarkably, the SO emission is not detected toward the dust trap down to our sensitivity limit (20 mJy/beam=2 K in a channel of 0.25 km s⁻¹), which proves the existence of a chemical differentiation within the dust trap. The excitation and radiative analysis carried out by [10] showed that the mean SO abundance towards the dust trap must be 2–3 times lower than in the rest of the disk to explain the observed morphology.

4 Chemical model

We used the time-dependent chemical model described by [9] to investigate the molecular chemistry in the dust trap. This model is an updated version of that reported by [1] and [6] and includes the elements H, C, N, O, and S. The initial molecular composition corresponds to that of a dark cloud ($n_{\text{H}}=2 \times 10^4$ cm⁻³, $T_k=10$ K) at a time of 0.1 Myr assuming the so-called “low metal” values [15] as initial abundances (M1 in [9]). The initial ionization fraction is

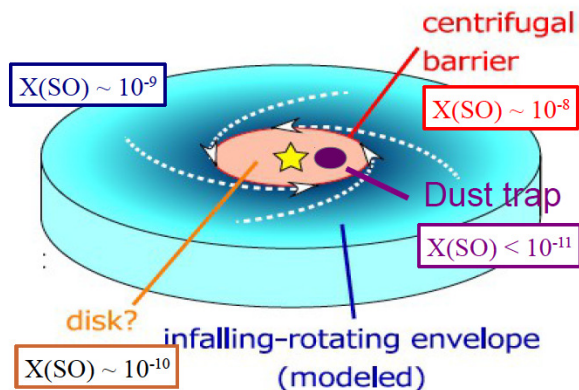


Figure 3: Illustrative scheme of the evolution of the SO abundance during the star/planet formation processes (adapted from [13]).

7×10^{-8} that is typical of dark cores ([4, 2]). We assume that the molecules are located close to the midplane and well shielded from the stellar UV radiation ($A_v > 10$ mag) and the gas and dust temperature is adopted equal to 45K. The value of the temperature is not relevant as long as $T \sim < 50\text{K}$, the SO evaporation temperature. In the model, all the grains have the same size. We vary the grain size, gas-to dust mass ratio and the molecular hydrogen density to investigate the effect of the dust trap on the molecular chemistry. Fig. 2 shows the CO, H₂CO and SO abundance as a function of time for different molecular hydrogen densities, gas-to dust mass ratios and grain sizes. The SO abundance presents variations of more than 3 orders of magnitude between 0.1 and a few Myr depending on the molecular hydrogen density. For high densities ($> 10^7 \text{ cm}^{-3}$), the SO abundance decreases to values $< 10^{-12}$ in less than 0.1 Myr. This is due to the adsorption of SO on dust grains and the rapid conversion of SO into SO₂ via the reaction $\text{SO} + \text{O} \rightarrow \text{SO}_2 + \text{photon}$. The desorption energy of SO₂ is higher (3070 K) than that of SO (desorption energy=2000 K) and once formed, is rapidly frozen onto the grain mantles. This result remains true regardless of the grain size and gas-to dust mass ratio (see Fig. 2). In contrast, the CO abundance is practically constant over time and is equal to the assumed initial C elemental abundance. On the basis of these calculations, the different CO, H₂CO, and SO spatial distributions are tracing the gas density structure within the disk. The SO abundance is very sensitive to the gas density and time evolution and is, therefore, a good tracer of the disk evolution.

5 Conclusions

We present high angular resolution interferometric images of the 1mm continuum, the ¹³CO J=2→1, C¹⁸O J=2→1, H₂CO J=3_{0,3} → 2_{0,2} and SO J=5₆ → 4₅ lines. Our data confirm that the SO emission comes from the transitional disk. However, sulfur monoxide (SO) presents an odd spatial distribution with lack of emission toward the dust trap. The SO abundance is very sensitive to the gas density and its lifetime in gas phase is less than 0.1 Myr for molecular hydrogen densities $> 10^7 \text{ cm}^{-3}$, typical of dust traps. This dramatic time dependency makes

this species a good tracer of the gas evolution (see Fig 3). Our high angular resolutions images show, for the first time, the chemical footprint of a dust trap in a transitional disk.

Acknowledgments

We thank the Spanish MINECO for funding support from grants CSD2009-00038, FIS2012-32096 and AYA2012-32032, and ERC under ERC-2013-SyG, G. A. 610256 NANOCOSMOS.

References

- [1] Agúndez, M., Cernicharo, J., & Goicoechea, J. R. 2008, *A&A*, 483, 831
- [2] Agúndez, M., & Wakelam, V. 2013, *Chem. Rev.*, 113, 871
- [3] van den Ancker, M. E., de Winter, D., & Tjin A Dje, H. R. E. 1998, *A&A*, 330, 145
- [4] Caselli, P., Walmsley, C. M., Terziewa, R., & Herbst, E. 1998, *ApJ*, 499, 23
- [5] Espaillat, C., Muzerolle, J., Najita, J., et al. 2014, *Protostars and Planets VI*, 49
- [6] Fuente, A., Cernicharo, J., Agúndez, M., et al. 2010, *A&A*, 524, A19
- [7] Hernández, J., Calvet, N., Briceo, C., Hartmann, L., & Berlind, P. 2004, *AJ*, 127, 1682
- [8] Oberg, K. I., Qi, C., Fogel, J. K. J., et al. 2011, *ApJ*, 734, 9
- [9] Pacheco-Vzquez, S., Fuente, A., Agndez, M., et al. 2015, *A&A*, 578, A8
- [10] Pacheco-Vzquez, S., Fuente, A., Baruteau, C., et al. 2016, *A&A*, 589, A60
- [11] Piétu, V., Guilloteau, S., & Dutrey, A. 2005, *A&A*, 443, 94
- [12] Rodríguez, L. F., Zapata, L. A., Dzib, S. A., et al. 2014, *ApJ*, 793, L2
- [13] Sakai, N., Oya, Y., Sakai, T., et al. 2014, *ApJ*, 791, L38
- [14] Tang, Y.-W., Guilloteau, S., Piétu, V., et al. 2012, *A&A*, 547, A84
- [15] Wiebe, D., Semenov, D., & Henning, T. 2003, *A&A*, 399, 197